View metadata, citation and similar papers at core.ac.uk

brought to you by CORE

provided by Repository@USM

CHARACTERIZATION OF INDIUM BASED LOW TEMPERATURE SOLDER ALLOY AND THE EFFECT ON SURFACE FINISH

ERVINA EFZAN BINTI MHD NOOR

UNIVERSITI SAINS MALAYSIA

JUNE 2013

CHARACTERIZATION OF INDIUM BASED LOW TEMPERATURE SOLDER ALLOY AND THE EFFECT ON SURFACE FINISH

by

ERVINA EFZAN BINTI MHD NOOR

Thesis submitted in fulfillment of requirements

for the degree of

Doctor of Philosophy

June 2013

Declaration

I declare that this thesis is the result of my own research, that it does not incorperote without acknowledgement any material submitted for a degree or diploma in any university and that it does not certain any materials previously published, written or produced by another person except where due reference is made in the text.

Signed :
Candidate's Name : Ervina Efzan binti Mhd Noor
Dated

Signed :
Supervisor's Name : Assoc. Prof. Dr. Zuhailawati binti Hussain
Dated

ACKNOWLEDGEMENTS

In the name of Allah, the most gracious and the most merciful and may his blessing be upon the prophet Muhammad (the blessings and peace of Allah be upon him).

I would like to sincerely express heartfelt gratitude to the invaluable assistance, guidance, and fruitful discussion of my supervisor, Assoc. Prof. Dr. Zuhailawati Hussain. I would like to express my deepest gratitude to co-supervisor, Assoc. Prof. Ahmad Badri Ismail and Dr. Nurulakmal Mohammed Sharif for their technical help, guidance and support.

I'm grateful to INTEL Technology and Universiti Sains Malaysia for financial support in CORT grant and RU Grant, which reflects their overwhelming in higher education and scientific research. I would like to express my appreciation to the School of Materials and Mineral Resources Engineering, Universiti Sains Malaysia for providing the necessary facilities for this project.

I would like to extend my grateful appreciation and thanks to Assc. Prof . Ir. Dr. Cheong Kuan Yew from School of Materials and Mineral Resources Engineering (USM) for his assistance, helpful advice and being there answering my endless questions. I would also like to pay immense tribute to the late Assoc. Prof. Dr. Luay Bakir Hussain Rahmatullah (1950-2008)–Universiti Sains Malaysia by dedicating this paper to his memory.

Special acknowledgement is given to all academic, administrative and technical staff of the School of Materials and Mineral Resources Engineering for their cooperative and friendly attitude that enabled this research to be carried out smoothly. I would like to acknowledge the help provided by Institute Postgraduate Studies.

Lastly, I would record a special word of thanks to my family for their endless support, patience and encouragement. I also wish to express my sincere thanks to my beloved husband who have given me his unfailing support and encouragement.

TABLE OF CONTENTS

ACKNOWLEDGEMENTS	III
TABLE OF CONTENTS	IV
LIST OF TABLES	X
LIST OF FIGURES	XII
LIST OF ABBREVIATIONS	IX
LIST OF PUBLICATIONS & SEMINARS	XXII
ABSTRAK	XXIV
ABSTRACT	XXV
CHAPTER ONE: INTRODUCTION	
1.1 Introduction	1
1.2 Problem Statement	4
1.3 Objectives of the Study	6
CHAPTER TWO: LITERATURE REVIEW	
2.1 Introduction	8
2.2 Soldering	8
2.3 Lead	10
2.4 Sn-Pb and Regulatory Trends for Leaded Solder	11
2.5 Lead-Free Solder and Its Requirement	12
2.6 Common Solder Electronic Assemblies	16
2.7 Phase Diagrams	19
2.7.1 Sn-Pb Phase Diagram	19
2.7.2 Bi-In Phase Diagram	20
2.7.3 Bi-Sn Phase Diagram	21
2.7.4 Bi-Cu Phase Diagram	21
2.7.5 Bi-Zn Phase Diagram	22
2.7.6 In-Sn Phase Diagram	23
2.7.7 In-Zn Phase Diagram	24
2.7.8 Cu-In Phase Diagram	25

2.7.10 Ag-Sn Phase Diagram 26
2.7.11 Sn-Cu Phase Diagram 27
2.7.12 Ag-Cu Phase Diagram 28
2.7.13 Sn-Ni Phase Diagram 29
2.6.14 Zn-Ni Phase Diagram 30
2.7.15 Cu-Zn Phase Diagram 31
2.7.16 In-Bi-Sn Phase Diagram 31
2.7.17 In-Bi-Zn Phase Diagram 32
2.8 Solder Density 33
2.9 Copper as interconnect material 34
2.10 Flux in soldering 34
2.11 Substrate material (surface finish) 35
2.11.1 Ni and Sn Coating 36
2.12 Reflow Soldering 37
2.13 Wetting Behaviours of Molten Solders 38
2.14 Soldering Wetting Measurements 40
2.14.1 Sessile Drop Method 40
2.14.2 Surface Tension of Molten Solder: Wetting Balance Method 43
2.15 Mechanical Properties of Solder Joints 48
2.15.1 Shear Test 49
2.16 Intermetallic Compound (IMC) 51
2.16.1 Intermetallic Formation on Cu Substrate 53
2.16.2 Intermetallic Formation on Ni and Sn Surface Finish 54

CHAPTER THREE: MATERIALS AND EXPERIMENTAL PROCEDURE
3.1 Raw Materials 57
3.1.1 Bismuth (Bi) 57
3.1.2 Indium (In) 57
3.1.3 Tin (Sn) 58
3.1.4 Zinc (Zn) 58
3.1.5 Copper (Cu) 59
3.1.6 Fluxes 59

3.2 Solder alloys 60
3.2.1 In-Bi-Sn (IBS) Ingot 60
3.2.2 In-Bi-Zn (IBZ) Ingot 60
3.3.3 Sn-Ag-Cu (SAC) alloy 61
3.4 Preparation of Copper (Cu) Substrate with Different Surface Finishes 62
3.4.1 Preparation of Ni/Cu Substrate 62
3.4.2 Preparation of Sn/Cu Substrate 63
3.5 Characterization of Solder Properties 64
3.5.1 Elemental Analysis of Solder by X-ray Fluorescence Technique 64
3.5.2 Melting Solder Temperature Measurement 64
3.5.3 Electrical Resistivity Measurement 65
3.5.4 Solder Density Measurement 65
3.5.5 Hardness Measurement 66
3.5.6 Phase Analysis by X-ray Diffraction 66
3.5.7 Microstructure Analysis under Scanning Electron Microscopy (SEM) 67
3.6 A study on Wettability and Interaction of Solder with Copper 67
3.6.1 Solder Wettability Using Sessile Drop (Spreading) Method 68
3.6.2 Solder Wettability Using Dipping Method 70
3.7 A Study on Wettability and Interaction of Solders with Nickel and Tin Surface Finish 71
3.8 Microstructure and Thickness of Intermetallic Between Solder and Substrate 72
3.9 Mechanical Properties 72
3.9.1 Mechanical Properties of Bulk Solder 72
3.9.2 Mechanical Test Using Shear 74
3.9.3 Fracture Surface 76

CHAPTER FOUR: RESULTS AND DISCUSSION
4.1 Characterization of Solders 77
4.1.1 XRF Analysis of In-Bi-Sn, In-Bi-Zn, and Sn-Ag-Cu Alloys 77

4.1.2 Differential Scanning Calorimetry Results 78
4.1.3 Electrical Measurement of In-Bi-Sn, In-Bi-Zn, and Sn-Ag-Cu 81
4.1.4 Density Solder Results 82
4.1.5 Hardness Test 84
4.1.6 Microstructure Analysis of Bulk Solders 84
4.1.7 X-ray Diffraction (XRD) analysis of Bulk Solders 88
4.2 Wettability of In-Bi-Sn and In-Bi-Zn on Cu Substrate with Different Surface Finishes 90
4.2.1 Spreading 91
4.2.2 Contact Angle of the In-Bi-Sn (IBS) and In-Bi-Zn (IBZ) Solders on Copper Substrates 96
4.2.3 The Effect of Different Surface Finishes on the Wettability of In-Bi-Sn (IBS) and In-Bi-Zn (IBZ) Solder Alloys 97
4.2.4 Wettability Using Dipping Method (Wetting Balance) 99
4.2.5 Effect of Different Surface Finish on T_0 and F_{max} at Temperatures on Cu Substrate 100
4.2.6 Effect of Surface Tension on Cu and Different Surface Finishes 109
4.3 Microstructure and Thickness of Intermetallic Between Solder and Substrate 113
4.3.1 Intermetallic Thickness Between Solder and Substrate 113
4.3.2 SEM and EDX analysis with XRD result 125
4.4 Mechanical Properties of Solder and Solder joints 147
4.4.1 Tensile Test for Bulk Solder 147
4.4.2 Effect of In-Bi-Sn and In-Bi-Zn at Different Temperatures on Cu Substrate Using Shear Test Method 147
4.4.3 Effect Ni and Sn surface finish on Shear Strength at Different Temperatures on Ni and Sn Using Shear Test 149
4.5 Fracture morphologies of different temperature on Cu substrate, Ni and Sn surface finish using shear test 151

CHAPTER FIVE: CONCLUSION AND FUTURE WORKS
5.1 Conclusion 161
5.2 Future Works 163

REFERENCES 164
APPENDIXES 183

LIST OF ABBREVIATIONS

DSC	Differential scanning calorimetry
EDX	Energy Dipersive X-ray
IBS	In-Bi-Sn
IBZ	In-Bi-Zn
IMC	Intermetallic compound
SAC	Sn-Ag-Cu
SEM	Scanning Electron Microscope
XRD	X-ray Diffraction X-ray Diffraction
XRF	X-ray fluorescence

LIST OF TABLES

Table 2.1 Common Compositions for Solder Alloys

Table 2.2 Density of Bulk Solder

Table 3.1Parameters Used for Melting Temperature Analysis

Table 4.1Elemental Compositions of Solder Alloys

Table 4.2 DSC results for In-Bi-Sn, In-Bi-Zn and Sn-Ag-Cu alloys

Table 4.3 Electrical Resistivity of the Solders Alloys and the pure metals

Table 4.4 Density of the Bulk Solders

Table 4.5 Density of elements Used in In-Bi-Sn and In-Bi-Zn Solders Alloys

Table 4.6 Density of Sn-based Solder Alloys

Table 4.7 Hardness Test (Vickers) for Solders

Table 4.8 Analysis Intermetallic Compound Using XRD

Table 4.9 Summary of Dipping Test Result on Wettability for In-Bi-Sn and In-Bi-Zn Solder System based on Wetting Time, Maximum Withdrawal Force and Surface Tension

Table 4.10 EDX Analysis for Points X and Y at 140 °C Reflow Temperature In-Bi-Zn Solder on Cu Substrate

Table 4.11 EDX Analysis for Points A and B at 140 °C Reflow Temperature In-Bi-Zn Solder on Cu Substrate

Table 4.12 EDX Analysis for Points A and B at 140 °C Reflow Temperature In-Bi-Sn Solder on Ni/Cu Substrate.

Table 4.13 EDX Analysis for Points C and D at 140 °C Reflow Temperature In-Bi-Zn Solder on Ni/Cu Substrate.

Table 4.14 EDX Analysis for Points C and D at 140°C Reflow Temperature In-Bi-Sn Solder on Sn/Cu Substrate.

Table 4.15 EDX Analysis for Points C and D at 140 °C Reflow Temperature In-Bi-Zn Solder on Sn/Cu Substrate

Table 4.16 Tensile Test for Bulk In-Bi-Sn and In-Bi-Zn Solders

LIST OF FIGURES

Figure 2.1. Printed wiring board (PWB)

Figure 2.2. Process of pin through hole and surface mount technology (SMT)

Figure 2.3. Sn-Pb phase diagram

Figure 2.4. Bi-In phase diagram

Figure 2.5.Bi-Sn phase diagram

Figure 2.6. Bi-Cu phase diagram

Figure 2.7: Bi-Zn phase diagram

Figure 2.8: In-Sn phase diagram

Figure 2.9: In-Zn phase diagram.

Figure 2.10: Cu-In phase diagram

Figure 2.11: Sn-Zn Phase Diagram

Figure 2.12: Ag-Sn phase diagram.

Figure 2.13: Cu-Sn phase diagram.

Figure 2.14: Ag-Cu phase diagram.

Figure 2.15: Sn-Ni phase diagram.

Figure 2.16: Zn-Ni phase diagram

Figure 2.17: Cu-Zn phase diagram

Figure 2.14: Ag-Cu phase diagram

Figure 2.15: Sn-Ni phase diagram

Figure 2.17: Cu-Zn phase diagram

Figure 2.18: In-Bi-Sn phase diagram

Figure 2.19: In-Bi-Zn phase diagram.

Figure 2.20. A schematic illustration of Cu position in interconnection. 1. heat sink, 2. Cu layer, 3. solder mask, 4. Micor via, 5. Solder ball, 6. Flux, 7 and 8. coating layer, 9. Cu pad, 10. Polymide

Figure 2.21. Commonly reflow profiles)

Figure 2.22. Relationship between contact angle and degree of wetting

Figure 2.23. Schematic of thermodynamic equilibrium in wetting

Figure 2.24. Typical wetting force curve obtained from wetting balance test

Figure 2.25. Typical wetting force curve obtained from wetting balance test

Figure 2.26. A typical nonwetting curve

Figure 2.27. Schematic of solder-substrate assembly for lap-shear test

Figure 2.28. Solder joints subjected to shear strain during thermal cycling due to CTE mismatch between the die, the solder, and the substrate

Figure 2.29: Schematic IMCs between solder and substrate

Figure 3.1: Flowchart of this research work

Figure 3.2: Bismuth

Figure 3.3: Indium

Figure 3.4: Tin

Figure 3.5: Zinc

Figure 3.6: Copper plate (a) with plastic and (b) after the plastic sticker was removed

Figure 3.7: Flux (zinc chloride)

Figure 3.8: Size of solder used for sessile drop method

Figure 3.9: Typical temperature profile for preparing the ingot

Figure 3.10: Sn-Ag-Cu commercial solder bar

Figure 3.11: Ni electroplating setup

Figure 3.12: Spreading test setup

Figure 3.13: Example of solder on copper substrate before spreading test

Figure 3.14: Example of measuring a spreading area in a spreading test

Figure 3.15: An example of contact angle measurement in spreading test

Figure 3.16: Schematic diagram of dipping test.

Figure 3.17: Solder dog-bone like shaped for tensile test

Figure 3.18: Direction of loading for tensile test of solder.

Figure 3.19: Setup for shear test specimen preparation

Figure 3.20: Example of soldered joint from (a) side view, (b) top view

Figure 3.21: Reflow temperature on hotplate and aluminium plate

Figure 3.22: Example of fracture surface using optical microscope

Figure 4.1: DSC for In-Bi-Sn

Figure 4.2: DSC for In-Bi-Zn

Figure 4.3: DSC for Sn-Ag-Cu

Figure 4.4: SEM for In-Bi-Sn solder at 1000X a) bright color (BiIn rich) b) dark color (Sn rich)

Figure 4.5: SEM for In-Bi-Zn with 1000X magnification with e) BiIn2 rich (brighter colour and f) Zn rich (dark colour)

Figure 4.6: SEM for Sn-Ag-Cu with 1000X magnification

Figure 4.7. Diffractogram of In-Bi-Sn bulk solder with the presence of BiIn intermetallic compound (ICDD 03-065-3890).

Figure 4.8. Diffractogram of In-Bi-Sn bulk solder with the presence of $BiIn_2$ intermetallic compound (ICDD00-007-0062).

Figure 4.9. Diffractogram of In-Bi-Sn bulk solder with the presence of Cu_6Sn_5 intermetallic compound (ICDD 03-065-23030).

Figure 4.10. Spreading area at different temperatures In-Bi-Sn(IBS) and In-Bi-Zn(IBZ) on Cu substrate.
Figure 4.11. Spreading area for In-Bi-Sn on copper substrate at different reflow temperatures: (a) 100 °C, b) 120 °C, and (c) 140 °C.

Figure 4.12. Spreading area for In-Bi-Zn on copper substrate at different reflow temperatures: (a) 100 °C, (b) 120 °C, and (c) 140 °C.

Figure 4.13. In-Bi-Sn (IBS) and In-Bi-Zn (IBZ) solder area at different temperatures on Ni and Sn coated copper substrates

Figure 4.14. Spreading area for In-Bi-Sn at different reflow temperatures: (a) 100 °C, (b) 120 °C, and (c) 140 °C on Ni substrate

Figure 4.15. Spreading area for In-Bi-Zn at different reflow temperatures: (a) 100 °C, (b) 120 °C, and (c) 140 °C on Ni substrate

Figure 4.16. Spreading area for In-Bi-Sn at different reflow temperatures: (a) 100 °C, (b) 120 °C, and (c) 140 °C on Sn substrate

Figure 4.17. Spreading area for In-Bi-Zn at different reflow temperatures: (a) 100 °C, (b) 120 °C, and (c) 140 °C on Sn substrate

Figure 4.18. In-Bi-Sn (IBS) and In-Bi-Zn (IBZ) solder areas at different temperatures on Cu, Ni/Cu and Sn/Cu substrate

Figure 4.19. Contact angle for In-Bi-Sn and In-Bi-Zn lead-free solder systems on Cu substrate at different reflow temperatures

Figure 4.20. Contact angle for In-Bi-Sn and In-Bi-Zn solders on Ni-coated Cu substrate at different temperatures

Figure 4.21. Contact angle for In-Bi-Sn and InBi-Zn solders on Sn-coated Cu substrate at different temperatures

Figure 4.22. Wetting time (sec) at different temperatures on copper substrate

Figure 4.23. Comparison wetting time in seconds at different temperaturesFigure 4.24. Example of wetting time (time cross zero) and maximum wetting force (Fmax) for In-Bi-Sn molten solder alloy with (a) Ni , (b) Sn, and (c) Cu substrates.

Figure 4.25. Example of wetting time (time cross zero) and maximum wetting force (Fmax) with (a) Ni, (b) Sn, and (c) Cu substrates

Figure 4.26. Maximum wetting force for In-Bi-Sn (IBS) and In-Bi-Zn (IBZ) with Cu substrate at different temperatures

Figure 4.27. Maximum wetting force for In-Bi-Sn (IBS) and In-Bi-Zn (IBZ) with Ni surface finish at different temperatures

Figure 4.28. Maximum wetting force for In-Bi-Sn (IBS) and In-Bi-Zn (IBZ) with Sn surface finish at different temperatures

Figure 4.29. Maximum wetting force for In-Bi-Sn (IBS) with various substrates at different temperatures

Figure 4.30. Maximum wetting force for In-Bi-Zn (IBZ) with various substrates at different temperatures

Figure 4.31. Surface tension for I-Bi-Sn (IBS) and In-Bi-Zn (IBZ) with Cu substrate at different temperatures

Figure 4.32. Surface tension for In-Bi-Sn (IBS) and In-Bi-Zn (IBZ) with Ni surface finish using different bath temperatures

Figure 4.33. Surface tension for In-Bi-Sn (IBS) and In-Bi-Zn (IBZ) with Sn surface finish using different bath temperatures

Figure 4.34. Back scattered electron (BSE) image of In-Bi-Sn/Cu joint at 100 °C (5K magnification)

Figure 4.35. Back scattered electron (BSE) images of In-Bi-Sn/Cu joint at 120 °C (5K magnification)

Figure 4.36. Back scattered electron (BSE) image of In-Bi-Sn/Cu joint at 140 °C (5K magnification)

Figure 4.37. Back scattered electron (BSE) image of In-Bi-Zn/Cu joint at 100 °C (5K magnification)

Figure 4.38. Back scattered electron (BSE) image of In-Bi-Zn/Cu joint at 120 °C (5K magnification).

Figure 4.39. Back scattered electron (BSE) image of In-Bi-Zn/Cu joint at 140°C (5K magnification)

Figure 4.40. Comparison of IMC thickness between In-Bi-Sn and In-Bi-Zn on Cu substrate at 100 °C, 120 °C, and 140 °C

Figure 4.41. Interfacial microstructure of In-Bi-Sn/Ni/Cu joint at 100 °C (5K magnification).

Figure 4.42. Interfacial microstructure of microstructure of In-Bi-Sn/Ni/Cu joint at 120 °C (5K magnification)

Figure 4.43. Interfacial microstructure of microstructure of In-Bi-Sn/Ni/Cu joint at 140 °C (5K magnification).

Figure 4.44. Interfacial microstructure of microstructure of In-Bi-Zn/Ni/Cu joint at 100 °C (5K magnification)

Figure 4.45. Interfacial microstructure of In-Bi-Zn/Ni/Cu joint at 120 °C (5K magnification).

Figure 4.46. Interfacial microstructure of In-Bi-Zn/Ni/Cu joint at 140 °C (5K magnification).

Figure 4.47. Interfacial microstructure of In-Bi-Sn/Sn/Cu joint at 100 °C (5K magnification)

Figure 4.48. Interfacial microstructure of In-Bi-Sn/Sn/Cu joint at 120 °C (5K magnification).

Figure 4.49. Interfacial microstructure of In-Bi-Sn/Sn/Cu joint at 140 °C (5K magnification)

Figure 4.50. Interfacial microstructure of In-Bi-Zn/Sn/Cu joint at 100 °C (5K magnification).

Figure 4.51. Interfacial microstructure of In-Bi-Zn/Sn/Cu joint at 120 °C (5K magnification)

Figure 4.52: Interfacial microstructure of In-Bi-Zn/Sn/Cu joint at 140°C (5K magnification)

Figure 4.53: IMC thickness for In-Bi-Sn (IBS) and In-Bi-Zn (IBZ) with Ni and Sn joint at different temperature

Figure 4.54. Interfacial microstructure at different reflow temperatures (a) 100 °C, (b) 120 °C, and (c) 140 °C (3000X) on In-Bi-Sn solder alloy.

Figure 4.55: Interface between In-Bi-Sn and Cu substrate at 1400C (5000X)

Figure 4.56: $Cu_{11}In_9$ intermetallic compound in In-Bi-Sn on Cu solder jointed at 140°C reflow

Figure 4.57: Cu_6Sn_5 intermetallic compound in In-Bi-Sn on Cu solder jointed at 140°C reflow

Figure 4.58: Interfacial microstructure at different reflow temperatures a) 100, b) 120 and c)140°C IBZ solder on Cu substrate

Figure 4.59: Interface between In-Bi-Zn and Cu substrate at 1400C

Figure 4.60: Cu5Zn8 intermetallic compound in In-Bi-Zn on Cu solder jointed at 140°C reflow

Figure 4.61: Cu11In9 intermetallic compound in In-Bi-Zn on Cu solder jointed at 140°C reflow

Figure 4.62. Interfacial microstructure at different reflow temperatures (a) 100 °C, (b) 120 °C, and (c) 140 °C In-Bi-Sn solder on Ni/Cu substrate

Figure 4.63. Interface between In-Bi-Sn solder on Ni/Cu substrate at 140 °C

Figure 4.64: $InNi_2$ intermetallic compound in In-Bi-Sn on Ni/Cu solder jointed at 140°C reflow.

Figure 4.65: Interfacial microstructure at different reflow temperatures a) 100, b) 120 and c)140°C In-Bi-Zn solder on Ni/Cu substrate

Figure 4.66: Interface between In-Bi-Zn and Ni/Cu substrate at 1400C (10K magnification)

Figure 4.67: $InNi_2$ intermetallic compound in In-Bi-Zn on Ni/Cu solder jointed at 140°C reflow

Figure 4.68: Interfacial microstructure at different reflow temperature a) 100, b) 120 and c)140°C In-Bi-Sn solder on Sn/Cu substrate

Figure 4.69: Interface between In-Bi-Sn solder on Sn/Cu substrate at 140°C

Figure 4.70: Cu_6Sn_5 intermetallic compound in In-Bi-Sn on Sn/Cu solder jointed at 140°C reflow

Figure 4.71: Cu11In9 intermetallic compound in In-Bi-Sn on Sn/Cu solder jointed at 140°C reflow

Figure 4.72: Interfacial microstructure at different reflow temperatures a) 100, b) 120 and c)140°C IBZ solder on Sn/Cu substrate

Figure 4.73. Interface between In-Bi-Zn and Cu substrate at 140°C
Figure 4.74: $Cu_{11}In_9$ intermetallic compound in In-Bi-Zn on Sn/Cu solder jointed at 140°C reflow

Figure 4.75: Cu_5Zn_8 intermetallic compound in In-Bi-Zn on Sn/Cu solder jointed at 140°C reflow

Figure 4.76. Shear strength on In-Bi-Sn(IBS) and In-Bi-Zn(IBZ) on Cu substrate at different temperature

Figure 4.77. Shear strength for In-Bi-Sn(IBS) and In-Bi-Zn(IBZ) on Ni surface finish at difference temperatures

Figure 4.78: Shear strength for In-Bi-Sn(IBS) on Sn surface finish at different temperature

Figure 4.79a: Fracture surface of In-Bi-Sn/Cu solder joint at 100ºC under optical microscope; a) upper and b) bottom.

Figure 4.79b: Fracture surface of In-Bi-Sn/Cu solder joint at 120ºC under optical microscope; a) upper and b) bottom.

Figure 4.79c: Fracture surface of In-Bi-Sn/Cu solder joint at 140ºC under optical microscope; a) upper and b) bottom.

Figure 4.80a: Fracture surface of In-Bi-Zn/Cu solder joint at 100ºC under optical microscope; a) upper and b) bottom.

Figure 4.80b: Fracture surface of In-Bi-Zn/Cu solder joint at 120ºC under optical microscope; a) upper and b) bottom.

Figure 4.80c: Fracture surface of In-Bi-Zn/Cu solder joint at 140ºC under optical microscope; a) upper and b) bottom.

Figure 4.81a: Fracture surface of In-Bi-Sn/Ni solder joint at 100ºC under optical microscope; a) upper and b) bottom.

Figure 4.82b: Fracture surface of In-Bi-Sn/Ni solder joint at 120ºC under optical microscope; a) upper and b) bottom.

Figure 4.83c: Fracture surface of In-Bi-Sn/Ni solder joint at 140ºC under optical microscope; a) upper and b) bottom.

Figure 4.84a: Fracture surface of In-Bi-Zn/Ni solder joint at 100ºC under optical microscope; a) upper and b) bottom.

Figure 4.84b: Fracture surface of In-Bi-Zn/Ni solder joint at 120ºC under optical microscope; a) upper and b) bottom.

Figure 4.84c: Fracture surface of In-Bi-Zn/Ni solder joint at 140ºC under optical microscope; a) upper and b) bottom.

Figure 4.85a: Fracture surface of In-Bi-Sn/Sn solder joint at 100ºC under optical microscope; a) upper and b) bottom.

Figure 4.85b: Fracture surface of In-Bi-Sn/Sn solder joint at 120ºC under optical microscope; a) upper and b) bottom.

Figure 4.85c: Fracture surface of In-Bi-Sn/Sn solder joint at 140ºC under optical microscope; a) upper and b) bottom.

Figure 4.86a: Fracture surface of In-Bi-Zn/Sn solder joint at 100ºC under optical microscope; a) upper and b) bottom.

Figure 4.86b: Fracture surface of In-Bi-Zn/Sn solder joint at 120ºC under optical microscope; a) upper and b) bottom.

Figure 4.86c: Fracture surface of In-Bi-Zn/Sn solder joint at 140ºC under optical microscope; a) upper and b) bottom.

LIST OF PUBLICATIONS & SEMINARS

Wettability and strength of In-Bi-Sn lead-free solder alloy on copper substrate, Ervina Efzan Mhd Noor , Ahmad Badri Ismail, Nurulakmal Mohd Sharif, Cheong Kuan Yuew , Tadashi Ariga, and Zuhailawati Hussain, Journal of Alloys and Compounds, Volume 507, Issue 1,2010 (I.F.2.20)

Low Temperature of Bi-In-Zn Lead-free Solder Alloy, Ervina Efzan Mhd Noor, Zuhailawati Hussain, Ahmad Badri Ismail, Nurulakmal Mohd Sharif, Tadashi Ariga, Material, Science & Technology (MS&T), pp. 124-131 (ISBN 13:978-1-61503-006-4).

Characteristic of Low Temperature of Bi-In-Sn Solder alloy, Ervina Efzan Mhd Noor, Ahmad Badri Ismail, Nurulakmal Mohd Sharif, Tadashi Ariga, and Zuhailawati Hussain, 33rd International Electronics Manufacturing Technology Conference 2008, Penang, IEEE Publishing art. no. 5507865

Interfacial Reaction of Bi-In-Zn/Cu and Bi-In-Zn/Ni solder joint alloy, Ervina Efzan Mhd Noor, Ahmad Badri Ismail, Nurulakmal Mohd Sharif, Kuan Yew Cheong, Tadashi Ariga, and Zuhailawati Hussain, 4th International Conference on Recent Advances in Materials, Mineral& Environment and 2nd Asian Symposium On Materials & Processing 2009, Bayview Hotel,Penang

Effect of temperature on the formation of Interfacial between Bi-In-Sn and Bi-In-Zn solders on Cu Substrate, Ervina Efzan Mhd Noor , Ahmad Badri Ismail, Nurulakmal Mohd Sharif, Cheong Kuan Yuew , Tadashi Ariga, and Zuhailawati Hussain, for 17TH EMSM SCIENTIFIC Conference 2008,Selangor

Contact Angle of Bi-In-Zn lead-free solder system on Cu and tin surface finish, Ervina Efzan Mhd Noor, , Zuhailawati Hussain, Nurulakmal Mohd Sharif, Cheong Kuan Yuew, Y.T.Chin, Tadashi Ariga, and Ahmad Badrii Ismail, International Conference of Science and Technology, UITM, 2009, Penang.

Effect of temperature on the formation of Interfacial between Bi-In-Sn solder on Cu and Ni Surface Finish, Ervina Efzan Mhd Noor , Ahmad Badri Ismail, Nurulakmal Mohd Sharif, Tadashi Ariga and Zuhailawati Hussain, Malaysian Metallurgical Conference 2008 (MMC 2008),UKM Selangor.

Surface Tension and Wetting Behaviour of Bi-In-Sn Alloys, Ervina Efzan Mhd Noor, Ahmad Badri Ismail, T.K. Soong, Y.T.Chin and Luay Bakir Hussain, NMC 2007, Johor Bahru, Malaysia.

Effect of Temperature on the Formation of the Interfacial Between In-Bi-Zn solder on Cu Substrates, Ervina Efzan Mhd Noor and Zuhailawati Hussain, Infineon Sysmposium 2011, Malacca

PENCIRIAN PATERI SUHU RENDAH BERASASKAN INDIUM DAN KESANNYA KE ATAS KEMASAN AKHIR

ABSTRAK

Peningkatan penggunaan peranti elektronik meningkatkan penggunaan pateri. Plumbum, bahan utama di dalam kebanyakkan pateri sangat merbahaya kepada kesihatan dan persekitaran. Oleh itu, penggantian pateri Sn-37Pb kepada pateri tanpa plumbum merupakan isu yang sangat penting di dalam industry elektronik. Oleh itu, perbandingan ciri-ciri pateri In-Bi-Sn dan In-Bi-Zn telah dilakukan. Analisis Pembezaan Pengubahsuaian Kalometri menunjukkan pateri In-Bi-Sn dan In-Bi-Zn menunjukkan takat lebur yang rendah masing-masing iaitu 61.3°C dan 72.3°C. Tegangan permukaan dan sudut sentuhan aloi pateri In-Bi-Sn dan In-Bi-Zn diukur pada substrat Cu dan pelbagai kemasan akhir pada suhu 100, 120 dan 140°C. Ukuran sessile drop menunjukkan sudut sentuhan bergantung kepada suhu aliran. Sudut sentuhan menurun perlahan dari 30.76° kepada 17.25° apabila suhu aliran meningkat dari 100 kepada 140°C bagi aloi pateri In-Bi-Sn dan In-Bi-Zn ke atas Cu substrat, pada julat 58° kepada 7° selepas pembasahan ke atas Ni/Cu substrat pada julat suhu aliran yang sama (100-140°C). Analisis Tenaga Penyerapan X-Ray menunjukkan dua lapisan sebatian antaramuka pada In-Bi-Sn Cu_6Sn_5 (berbentuk scallop) dan $Cu_{11}In_9$ (warna cerah) ke atas substrat Cu dan Sn/Cu. Sebatian antaramuka antara aloi pateri In-Bi-Zn boleh dilihat adalah Cu_5Zn_8 (sambungan satah) dan sedikit lapisan $Cu_{11}In_9$ ke atas substrat Cu dan Sn/Cu. Walaubagaimanapun, hanya terdapat satu sebatian antaramuka terbentuk pada kedua-dua pateri (In-Bi-Sn dan In-Bi-Zn) ke atas substrat Ni/Cu iaitu $InNi_2$. Semakin suhu aliran meningkat, kekuatan ricih pada pateri In-Bi-Sn dan In-Bi-Zn ke atas Cu, Ni/Cu dan Sn/Cu juga meningkat disebabkan sudut sentuhan yang berkurangan dan perebakan kawasan yang besar.

CHARACTERIZATION OF INDIUM BASED LOW TEMPERATURE SOLDER ALLOY AND THE EFFECT ON SURFACE FINISH

ABSTRACT

The increased use of electronic devices has increased the usage of solder connections. Lead, the prime solder hitherto used, is hazardous to human health and the environment. Thus, replacing Sn-37Pb with a lead-free solder is one of the most important issues in the electronics industry. As such, the characteristics of In-Bi-Sn and In-Bi-Zn compared with that of the Sn-Ag-Cu solder alloy were studied. In the differential scanning calometry analysis, In-Bi-Sn and In-Bi-Zn system alloys presented a low melting temperature of 61.3 °C and 72.3 °C, respectively. Surface tension and contact angle of In-Bi-Sn and In-Bi-Zn lead-free solder alloys were measured on Cu substrate and different surface finishes at 100, 120 and 140 °C reflow. Sessile drop measurements showed that the contact angle depended on the reflow temperature. The contact angle gradually decreased from 30.76° to 17.25° as reflow temperature increased from 100 to 140 °C and for In-Bi-Sn and In-Bi-Zn solder alloy on Cu substrate, ranged from 58° to 7° after wetting on Ni/Cu substrate at the same reflow temperature range (100 to 140°C). Energy-dispersive X-ray analysis found two layers of intermetallic compound in the In-Bi-Sn solder alloy: Cu_6Sn_5 and $Cu_{11}In_9$ (scallop shaped) and $Cu_{11}In_9$ (brightly coloured) with Cu and Sn/Cu substrate. The IMC between the In-Bi-Zn solder alloy could be observed: Cu_5Zn_8 (continuous planar) and $Cu_{11}In_9$, a minor IMC layer with Cu and Sn/Cu substrate. However, only one type of IMC was formed between both solders (In-Bi-Sn and In-Bi-Zn) and Ni/Cu substrate, which was $InNi_2$. As the reflow temperature increased, the shear strength of the In-Bi-Sn and In-Bi-Zn solder alloys on Cu, Ni/Cu and Sn/Cu joints improved due to reduced contact angle and larger spreading area.

CHAPTER 1

INTRODUCTION

1.1 Introduction

Miniaturization is a key issue in achieving advanced performance from electronic devices. Rapid advances in microelectronic design and technology in recent decades have made modern day electrical and electronic equipment (EEE) obsolete within a very short period after their purchase resulting in mountains of electronic waste (e-waste) to be dealt with in many countries around the world. According to a United Nations estimate, collectively the world generates 20 to 50 million tons of e-waste every year (Schwarzer et al., 2005). The growing consumer demand and discarded electrical and electronic products (often called e-waste) has been estimated to already constitute 8% of municipal waste (Tsydenova & Bengtsson, 2011).

E-waste contains significant quantities of toxic materials, considered dangerous, as certain components of some of these electronic products contain materials such as lead, which are hazardous, depending on their condition and density. Consumer electronics devices (CEDs) contain numerous toxic materials, such as mercury, lead, zinc, and cadmium, which pose a threat to public and environmental health if CEDs are improperly discarded. These include metals such as lead, mercury, cadmium; and chemicals such as polychlorinated biphenyls. Among these metals, lead is one of major concern because of the extensive use of lead solder, especially eutectic tin-lead (Sn-37Pb) or near eutectic Sn-40Pb solder in the assembly of the modern electronic circuits (Saphores et al., 2009a).

Lead (Pb) containing solders have been widely used in the electronics industries for a long time due to its good solderability, low melting temperature, and satisfactory mechanical properties. It serves to form interconnections between electronic components and printed circuit boards (PCB) both electrically and mechanically (Chen et al., 2005). However, the presence of lead raises several environmental concerns, including the fate of the lead upon disposal of the discarded electronic device. The toxicity characteristic leaching procedure (TCLP) is the United State Environmental Protection Agency's (US EPA) method used to determine the status of a solid waste as a hazardous waste due to the toxicity characteristic (TC) (Timothy et al., 2008).

The European Parliament and the Council of the European Union (EU) adopted the Directive on the "Restriction of the Use of Hazardous Substances" (RoHS) (2002/95/EC) on 23 January 2003. This Directive bans certain hazardous substances in electrical and electronic equipment. It covers a broad range of uses for toxic chemicals, with three articles specifically addressing lead, as shown in the sidebar. Additionally, the European Union (EU) Directive 2002/95/EC—Restriction of Hazardous Substances (RoHS) restricts the use of specific hazardous materials found in electrical and electronic products including lead beginning 1 July 2006. Waste Electrical and Electronic Equipment Directive (WEEE Directive) mandates the producers of electrical and electronic equipment to finance the collection, recycling, or otherwise adopt nonhazardous disposal of their products after consumers are ready to discard them (Ogunseitan, 2007).

In Japan, Japanese law mandates the take-back of various household electrical appliances to reuse and recycle materials and substances in those electrical

appliances. Japanese Electronic Industry Development Institute Association (JEIDA) and Japanese Institute of Electronic Packaging (JIEP) followed the same steps to maintain trade with EU countries and marketing edge by promoting "green product" (lead-free) to their customers.

For these reasons, environmental regulations in various countries have emerged. Following the impetus of the EU directives, Japan (Kim et al., 2005a), China (Anonymous, 2006), and South Korea (Ogunseitan, 2007) have instituted similar regulations to limit the use of lead and other RoHS toxicants in electronic and electrical equipment. Although binary, ternary, and quaternary systems in solder investigated showed improving properties, none have met all standards, which included a low melting temperature, wettability, mechanical performance, and good manufacturability (Suganuma, 2001). Therefore, research on lead-free solders remains an important issue in the electronic industry (Abtew & Selvaduray, 2000; McCormack & Jin, 1994).

Therefore, an alternative solder free from Pb needs to be developed. For example, Sn–Ag solder alloy (melting temperature, 221 °C) and Sn–Ag–Cu solder alloy (melting temperature, 217 °C) have been investigated as replacements (Buyok & Maras, 2009). However, despite the general acceptance of these solders as the leading Pb free solders, they have a number of disadvantages, one of which is a relatively high melting temperature. High melting temperature requires high reflow temperature. Thus, low melting temperature solder is more suitable for an alternative solder.

Lowering reflow temperatures reduces thermal stress on adjacent components. In addition, heat-sensitive materials such as ferroelectric polymers or liquid crystals

are increasingly introduced to integrated chips. These heat sensitive materials, in general, have limited thermal stabilities and some of them require low-temperature assembly of below 125 °C (Suh et al., 2008).

The metallurgical behaviour of low reflow temperatures solder joints with different surface finishes (Ni and Sn) and the related reliability of joints on surface finishes have not been sufficiently studied yet. Therefore, the present study was carried out to investigate the reliability of In-Bi-Sn and In-Bi-Zn solders with Cu substrate and various surface finishes.

1.2 Problem Statement

Among the six prohibited substances in the RoHS directive, the prohibition of lead has had the largest impact on the electronics industry. In response to the need to adopt lead-free process technology, companies have variously switched to other substitute alloys. Most companies in the industry have switched to a tin-based lead-free solder in recent years, and added other metals to reinforce solder characteristics. Numerous types of lead-free alloys are currently available in the market (Lin et al., 2007; Liou et al., 2009; Wang et al., 2008a; Yoon et al., 2009). Of these, Sn-Ag-Cu alloys are widely used in Europe, in the US, and in Japan.

Despite of the general acceptance of Sn-Ag (221 °C) and Sn–Ag–Cu solder alloy (217 °C)(free lead), the disadvantages of these alloys, which could not be ignored are the high melting points. A higher melting point leads to a 20–30 ◦C increase in the peak reflow temperature required for assembly compared with that required for Pb-Sn eutectic solder. Such an increased temperature is detrimental to many microelectronic components, making assembly very difficult. The increased

temperature reduces the integrity, reliability, and functionality of printed wiring boards (PWBs) and their other components (Kim et al., 2004).

Another alternative is Sn-Zn solder alloy (Zn about 9wt%) with a melting point of about 198 °C (Garcia et al., 2010; Hu et al., 2010; Mahmudi et al., 2009). This alloy offers significant benefits in terms of cost and good mechanical properties (Mahmudi et al., 2009; Garcia et al., 2010). However, this alloy suffers from low oxidation resistance and poor wettability (Mahmudi et al., 2009).

Despite of the development of Sn-Ag, Sn-Ag-Cu and Sn-Zn solders, the properties of these solders are still not good enough for these alloys to be employed in temperature-sensitive components, optoelectronics modules, step soldering processes, and thin printed wiring boards (PWBs) (Suganuma, 2004), all of which require a low melting temperature. Low-temperature soldering is necessary when electronic devices to be soldered are prone to thermal damage.

Although lead-free solder have been extensively studied, information about the In-31.6Bi-19.6Sn (In-Bi-Sn) and In-32.7Bi-0.5Zn (In-Bi-Zn) solders alloys are not yet available in the literature. Since In-Bi-Sn and In-Bi-Zn solder alloys have low liquidus temperature, it may be used for low-temperature soldering. Furthermore, its low liquidus temperature suits for use as an organic-based transistor such as liquid crystal display (145-178 °C), in the new generation of nano silicon chips (100-300 °C), and in polymeric conductive boards (140-400 °C). Using these alloys, outer space nano satellites to be used under cryogenic conditions (minus 147-447 °C) can be manufactured at low temperatures.

Compared with Sn-based solders, In-based solders possess advantages such as lower melting points, better wettability, and longer fatigue life (Chuang et al., 2009). Step-soldering, required for high-density packaging of multichip modules (MCMs), uses a number of solders with wide range of melting points. Indium was used as the joining material because it remains electrically conductive and ductile to cryogenic temperatures and helps relieve the strain between the substrate and the package (Chang & McCluskey, 2009).

The presence of intermetallic compounds (IMCs) between solder alloys and the surface finishes ensures a good metallurgical bonding. Thus, many studies have been performed on the joint reliability and interfacial reaction between lead free solders and various surface finishes such as Ni and Sn (Gosh et al., 2000; Koo et al., 2005; Sharif et al., 2004; Yoon et al., 2009). Nevertheless, studies on the interfacial reactions and mechanical properties of In-Bi-Sn and In-Bi-Zn solder on Ni and Sn surface finish have not been available yet in the literature.

1.3 Objectives of the Study

In this work, the properties of In-Bi-Sn and In-Bi-Zn solder alloys were investigated.

The main objectives of this work include:

1. To develop and characterize physical properties of In-Bi-Sn and In-Bi-Zn new solders in terms of melting temperature, density, and microstructure.

2. To study the wetting characteristic of the new solders on Cu, Ni, Sn coated surface finishes at different reflow temperatures.

3. To study the reliability of the new solder on Cu, Ni, Sn coated surface finishes by measuring shear properties of the joint.

CHAPTER 2

LITERATURE REVIEW

2.1 Introduction

Joining processes, such as attaching two or more substrates or base materials, be they metals, ceramics, or plastics, can be considered as one of two generalized methodologies: filler material joining or fusion joining (Vianco, 1999a).

2.2 Soldering

The American Welding Society defines soldering as a joining process where a coalescence between metal parts is produced by heating to temperature below 425 °C using filler metals (solders) having melting temperatures below those of the base metal (Frear et al., 1994). Manko (2001) defined soldering as a metallurgical joining method using filler metal (the solder) with a melting point below 315 °C. Metallurgical bonds are connections between metals only (Manko, 2001). In general, they are those bonds in which metallic continuity from one metal to another is established. The roles of solder, the reaction itself is exothermic which means that it requires no energy input to proceed, once it has started. Soldering heat is needed to melt the solder, because solid solder can neither react with the substrate (or only very slow), nor flow into a joint (Strauss, 1998). Various types of solder have been used in the electronic industry lately. Examples are such as lead solder, hard solder, flux core solder, and lead-free solder. Previously, lead solder is the most widely used in the electronic industry, however, due to the toxicity of lead (Pb) present, alternative solders need to be considered (Yoon et al., 2008).

There are two levels of packaging where solders are used in electronics assembly. One of the levels is the bonding of the die (Chip) to a substrate, which is known as Level 1 packaging (Abtew & Selvaduray, 2000). In Level 2 packaging, the components are mounted in printed wiring board (PWB). A printed circuit board is used to connect electrically and mechanically to hold the electronic components using conductive pathways (Anonymous, 2009a). Figure 2.1 shows an actual PWB (Anonymous, 2010a). The two ways to connect the electronic equipment to the PWBs are pin through hole and surface mount technology (SMT). A graphical representation of the processes of pin through hole and SMT are shown in Figure 2.2 (Anonymous, 2009a).

Figure 2.1. Printed wiring board (PWB)

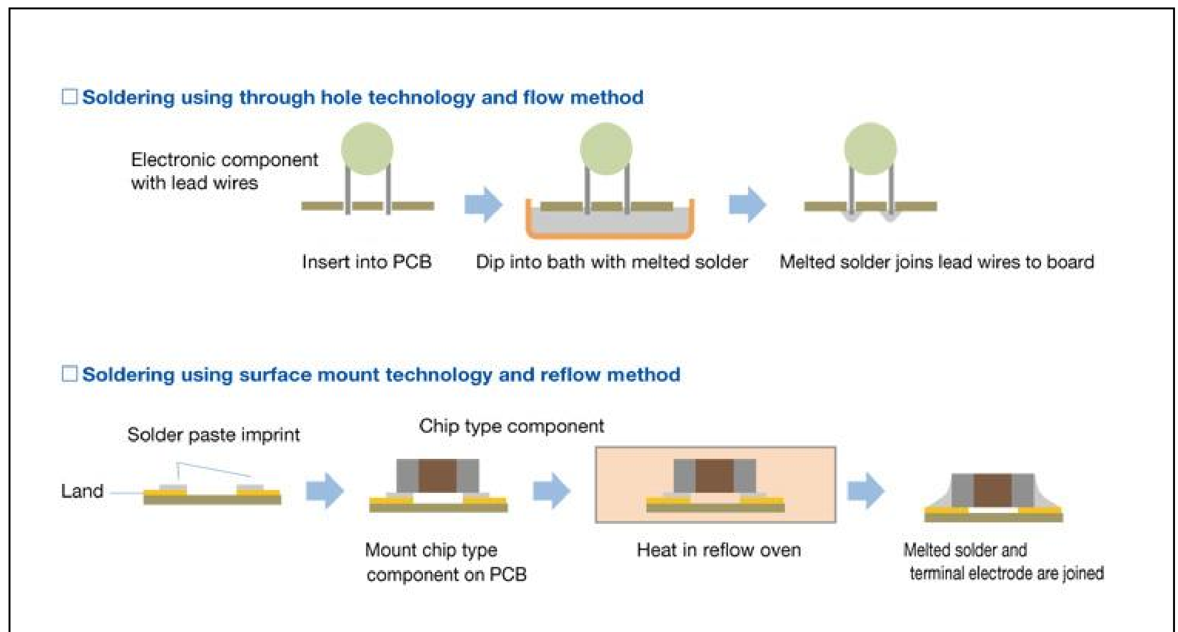

Figure 2.2. Process of pin through hole and surface mount technology (SMT) (Anonymous, 2010a)

2.3 Lead

Lead is a heavy metal found naturally in the earth that has been used in many ways for hundreds of years. Lead's atomic number may not be 1 (it is 82) but it ranks near the top when comes to industrial uses (Casas & Sordo, 2006). Lead (and its compounds) have been cited by the Environmental Protection Agency (EPA) as one of the top 17 chemicals posing the greatest threat to human life and the environment (Abtew & Selvaduray, 2000). Although lead is very soft in its pure state and can be scratched even with the fingernail, small additions of impurities such as antimony, arsenic, copper, zinc, and so forth, would make the lead much harder by solution hardening. These small traces of elements are enough to increase the hardness and strength appreciably (Manko, 2001).

Health concerns are relatively recent, and they came with the realization that very small amounts of lead have a profound effect on the human body. Lead binds strongly to proteins in the body and inhibits normal processing and functions of the human body (Abtew & Selvaduray, 2000). The common types of lead poisoning may be classified according to (a) alimentary, (b) neuromotor, and (c) encephalic. Lead poisoning commonly occurs following prolonged exposure to lead or lead compounds. The damage is often induced slowly (Braga et al., 2007; Lee, 2001).

In industry, the authorities have allowed lead containing dross, clippings, spent solder, and the like, to be recycled and not classified as "hazardous waste." However, still one lead-containing material has not been addressed by the cycle, namely discarded products such as electronics equipment which end up in the landfill (Manko, 2001).

2.4 Sn-Pb and Regulatory Trends for Leaded Solder

The term solder has become synonymous with the tin-lead system and widely used in the industry. The lead solder alloys most commonly used for electronics assembly contain tin (Sn) as a main composition with a standard eutectic composition being Sn63Pb37. These alloys consist of 60% tin (Sn) and 37% lead (Pb). The eutectic ratio of 63/37 corresponds closely to a formation of α and β eutectic compound.

Sn–Pb solders for metal interconnections have appreciated since at least Roman times, dating back to 2000 years ago. These solder materials serve as electrical, thermal, and mechanical connectors in Surface Mount Technology (SMT), such as ball grid arrays (BGAs), chip scale packages (CSPs), and flip chips (FCs)

(Lun, 2001). The development of compositions alloy developed provides many benefits, such as ease of handling, low melting temperatures, good workability, ductility, relatively inexpensive to produce, and using superior wettability and spreading characteristics on Cu and its alloys (Chen et al., 2006; Humpston & Jacobson, 2004; Kanchanomai et al., 2002; Suganuma, 2001).

In the electronics industry, the lead generated by the disposal of electronic assemblies is considered as hazardous to the environment (Abtew & Selvaduray, 2000). The elimination of lead from electronic devices as mandated by Restriction of Hazardous Substances (RoHS) is changing the playing field for all those involved in the printed circuit industry (Satyanarayan et al., 2011). The attempt to ban lead from electronic solder was initiated in the U.S. Congress. The European Union (EU) and RoHS set stringent limits on the amount of hazardous materials that could be present in electronics products. This has speeded up the market for a lead-free soldering system (Xin, 2007). Major Japanese companies also set voluntary timetable for the phasing out of lead (Wu et al., 2004).

On the PCB level, OEMs have the brunt of dealing with the change that designers are always pushing the limits of the industry's capabilities to meet the requirements of their newer designs (Milad & Orduz, 2007).

2.5 Lead-Free Solder and Its Requirement

Lead-free solder in the electronics industry is a segment of a global trend towards a lead-free environment, although the lead used in electronics soldering accounts for less than 1% of the total industrial use of this metal (Xin, 2007). To become a good solder material, lead-free solder needs to be reliable over long-term

use (Wu et al., 2004). The current processing equipment and conditions for electronics assembly are optimized for Sn–Pb solders. Any new conditions for lead-free alloys must ensure both productivity and reliability at least equivalent to the present level of Sn–Pb solders (Suganuma, 2001).

There are strict performance requirements for solder alloys used in microelectronics. According to Kang (2001), there are several requirements for new lead-free solder alloy to replace the lead solder Sn-Pb (Kang, 2001). In general, the solder alloy must meet the expected levels of electrical and mechanical performance, whist at the same time it must also have the desired melting temperature (Abtew & Selvaduray, 2000). One of the most sensitive eutectic solder systems parameter for the quality of soldered joints is soldering temperature (Suganuma, 2001). It must adequately wet common printed circuit board (PCB) lands, form inspectable solder joints, allow high volume soldering and rework of defective joints, provide reliable solder joints under service conditions, and it must not significantly increase assembly cost (Abtew & Selvaduray, 2000).

When trying to identify an alternative to the current Sn-Pb solders that are widely used, it is important to ensure that the properties of the replacement solder are comparable to or superior to Sn-Pb solders. The first step in finding suitable alloy candidates is to search for some nontoxic, low-melting temperature alloys that can replace this amount of Pb (Suganuma, 2001). The search for a global Pb-free replacement for Sn-Pb eutectic alloy has been an evolving process as the threat of a regional lead ban became a reality in July 2006.

The properties of solders that are important from a manufacturing and a long-term reliability standpoint are listed as in the following:

(a) Non- toxic

The main driving force for elimination of Pb is its toxic nature (Mayappan, 2007). The concern here is not just the toxicity of Pb; but the fact that when disposed of in landfills, Pb can eventually leach out and can contaminate underground water sources and subsequently finds its way into the human ecosystem in an ingestible form. In choosing alternatives for Pb, it must be ascertained ahead of time that the alternatives will not pose a similar hazard (Abtew & Selvaduray, 2000; Jasbir, 2007; Suganuma, 2001; Wu et al., 2004).

(b) Melting Temperature

The temperature margin beyond the melting temperature of solder is about 50 °C for reflow soldering (Abtew & Selvaduray, 2000). At present, some of the electronic components (such as capacitors and connectors) cannot withstand an increase in reflow temperature need to modify or develop processing conditions to incorporate heat-resistant components (Suganuma, 2001). The solder must also have a liquidus temperature below the melting point (solder temperature) of the parent materials and any surface metallization.

(c) Narrow pasty range

The pasty range is the temperature range between solidus and liquidus, where alloy is part solid and part liquid. When the pasty range is narrow, the solder needs shorter time to solidify. The acceptable level for pasty range is less than 30 °C by National Center for Manufacturing Science (NCMS). The Centre completed its lead-free solder project in 1997 (Jasbir, 2007).

(d) Acceptable wettability

Wettability behaviour is important to the interconnection of electronic packages like soldering (Wu et al., 2004). In reflow step, the molten solder contacts the substrate, wet the substrate, causing an interfacial reaction (Chen, 2010). This is necessary to allow capillary action to take place to fill a joint gap or to fill a plated-through hole (PTH) in a printed wiring board during soldering (Evans, 2007).

(e) Process economy

Cost is another important factor in the adoption of solders for practical electronic applications (Satyanarayan & Prabu, 2011). The microelectronics industry, wherever, is extremely cost conscious, and the industry is not willing to overlook increased costs; thus, higher-priced proprietary alloys will not be accepted. The history of the industry has been to produce continuously at higher performance with lower costs. Cost competitiveness in the electronics industry is maintained by reducing the cost of individual components to a minimum to maximize the overall cost reduction. In general, taking cost of raw metals into consideration, most lead-free solders cost about two to three times more than Sn–Pb solders (Suganuma, 2001). From a purely cost standpoint, an unpatented solder alloy, with multiple suppliers, with a stable price structure, and without geopolitical concerns, would be most desirable.

(f) Material manufacturability and acceptable processing temperature

Solder alloys must be compatible with standard surface finishes used today or have a universally acceptable finish of their own. This is a critical point used to having terminations finished with solderable coatings such as gold, platinum, silver, copper, and the solder itself. The solder alloy system must be stable and form as few intermetallic compounds as possible. The intermetallic compound (IMC) should not pose an embrittlement problem in the solder and the wetted interface (Manko, 2001).

The temperature range for processing temperature has to be good with hardware built, components, and substrates used. The lower temperatures would be acceptable for low-end commercial applications.

(g) Form reliable joints

One of the major concerns of area array packages, such as ball-grid-array (BGA) and flip chip, is the reliability of the solder joint (Hwang et al., 2004). Solder properties are important to solder-joint integrity in surface mount technology (Zeng & Tu, 2002). Recent studies have indicated that the interfacial intermetallic compounds (IMCs) between solder alloys and substrates have a significant effect on the reliability of solder joints (Yoon & Jung, 2006).

2.6 Common Solder Electronic Assemblies

There are three important considerations in the selection of solder alloys. They are the composition, the solidus temperature, and the liquidus temperature. The composition of the alloy has a direct effect on the joint strength and the wettability of the solder (Cheng et al., 2009; Chria & Ozvold, 2008). It is also a crucial factor in

determining whether the alloy is a suitable replacement as a lead-free solder. The solidus temperature is the point where 100% of the alloy is in solid crystals. The liquidus temperature is the point where 100% of the alloy is in liquid form (Chria & Ozvold, 2008). The solid and liquid phase will coexist when the temperature is in between the solidus and the liquidus temperature. The solder alloy is aeutectic alloy when the liquidus and the solidus temperature are the same (Kim et al., 2004).

A relatively large number of lead-free solders have been proposed, and they are summarized in Table 2.1 with their elemental compositions and melting temperatures. The melting temperatures are present in the solidus, Ts, liquidus, Tl, and eutectic temperatures, Te. The solder alloys are binary and ternary.

Since the properties of the binary lead-free solders cannot achieve the requirements, the ternary and quarternary lead-free solders have been developed by the addition of alloying elements to the binary lead-free solders to improve the performance (Anderson et al., 2001). Many of the systems are based on adding small quantities of a third or fourth element to binary alloy systems to lower the melting point and increase wetting and reliability. With increasing amount of additive elements, (a) the melting point of system decreases, (b)the bond strength first rapidly decreases, then almost levels off, then decreases again, and (c) the wettability increases rapidly first, reaching the maximum at composition corresponding to mid-point of plateau of bond strength, then decreases (Lee, 2001). Various compositions can be formulated from the combination of the major elements: Sn, Ag, Cu, Bi, In Sb, and Zn in binary, ternary, or multicomponent systems (Abtew & Selvaduray, 2000; Kucharski & Fima, 2005; Lin et al., 2008; Moelans et al., 2003). Meanwhile, elements such as gold (Au) (Yoon et al., 2008), ferum (Fe)(Wang, 2009), germanium

(Ge) (Yen et al., 2011), lithium (La) (Shiue & Chuang, 2010),, gallium (Ga) (Chen et al., 2010), magnesium (Mg), and nickel (Ni) can be added in a very small portion to refine the grain or strengthening mechanisms (Wu et al., 2003) (Wang et al., 2008).

Table 2.1 *Common Compositions for Solder Alloys*

Solder alloy, wt%	**Solidus/liquidus temperature**		
	ºC	**ºF**	**Pattern**
52In-48Sn	118/118	244/244	Indium
50In-50Sn	118/125	244/257	Indium
58Bi-42Sn	138/138	281/281	-
67Bi-33In	109/109	228/228	Indium
43Sn-43Pb-14Bi	143/163	289/325	Indium
58Sn-42In	118/145	244.4/293	Indium
97In-3Ag	143/143	289/289	
63Sn--37Pb	183/183	361/361	(Control)
60Sn-40Pb	183/190	361/374	
96.5Sn-3.5Ag	233/240	451/464	Indium
80Sn-10In-10Bi	153/199	307.4/390.2	IBM
87Sn-8Zn-5In	175/188	347/370.4	AT&T

Note. Adapted from *Lead-Free Soldering* (p. 20-30), by A. A. Jasbir, 2007, New York: Springer Science+Bussiness Media, LLC.

For binary and higher systems, a unique "melting temperature" can be expected only for eutectic compositions or for compositions that melt congruently. Other compositions can be expected to melt over a range of temperatures, with melting beginning at the solidus temperature and being complete at the liquidus temperature. Elements such as Bi, Cd, In, Zn, Au, Ti, Ga, Hg, Cu, Sb, and Ag are the candidates that can lower the melting temperature of Sn which is important to develop solder alloys that possess the require properties for electronic packaging and assembly (Braga et al., 2007; Hwang & Suganuma, 2004).

2.7 Phase Diagrams

Phase diagram is the keyword for initial selection of candidate solders and interaction between solder and substrate especially in wetting and spreading. The understanding of phase diagrams for alloy system is extremely important because there is a strong correlation between microstructure and mechanical properties. The development of microstructure of an alloy is related to characteristics of its phase diagram. In addition, the phase diagram is also frequently used to analyze the melting point or eutectic point of a multi-components system (Zhang et al., 2004).

2.7.1 Sn-Pb Phase Diagram

The binary phase diagram for Sn-Pb is a typical and a very well-known phase diagram. The most popular is 40Sn-60Pb. Figure 2.3 shows the Sn-Pb phase diagram. In industry, solders are called tin-lead.

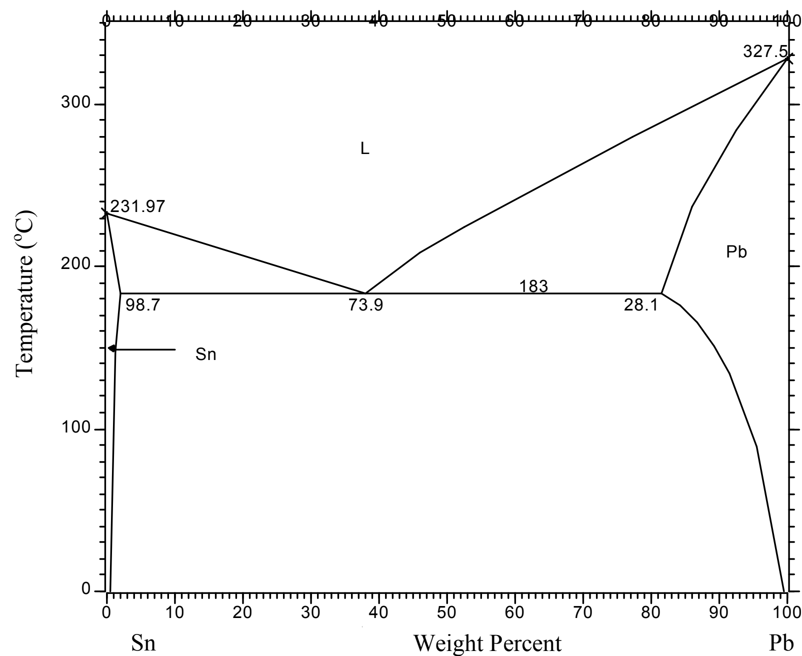

Figure 2.3. Sn-Pb phase diagram (Massalski, 1990).

The temperature of 183 ºC is the eutectic temperature, T_{eut}, of the binary Sn-Pb system. At 183 ºC, complete solidification takes place. At temperature a fraction of a degree lower than 183 ºC, the solder comprises two solid phases: Sn-rich phase designated by ß, having a composition 97.5 Sn and Pb-rich phase, α, having a composition 19Sn-81Pb.

2.7.2 Bi-In Phase Diagram

Four stable intermediate phases exist: (1) Bi-In, with a congruent melting point of 109.7 ºC; (2) Bi_3-In_5, with peritectic melting point of 88.9 ºC; (3) Bi-In_2, melting congruently at 89.5 ºC; and (4) In-type ε, existing between 93.5 and 49 ºC (Okamoto, 1990). Figure 2.4 shows Bi-In phase diagram.

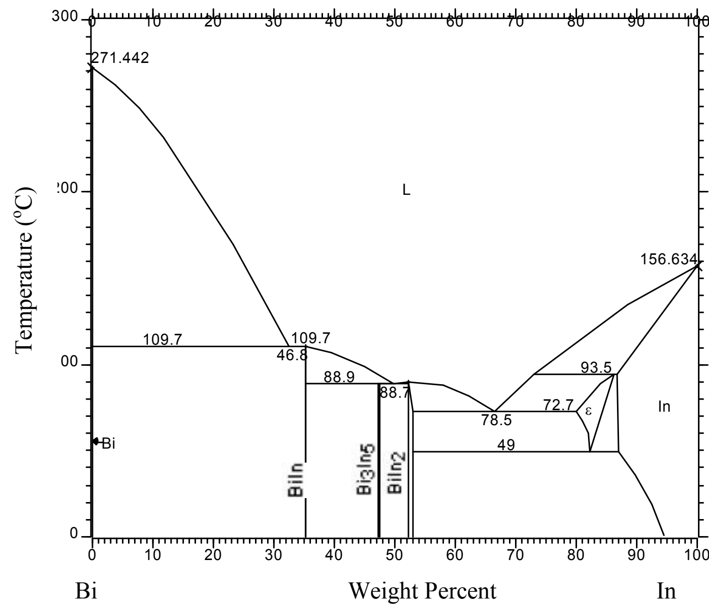

Figure 2.4. Bi-In phase diagram (Okamoto, 1990)

2.7.3 Bi-Sn Phase Diagram

Figure 2.5 shows that the Sn–Bi alloy has a eutectic composition of 42Sn–58Bi and a relatively low eutectic temperature of 139 °C. The room temperature equilibrium phases are Bi and Sn with about 4 wt.% Bi in solid solution (Mei & Morris, 1992).

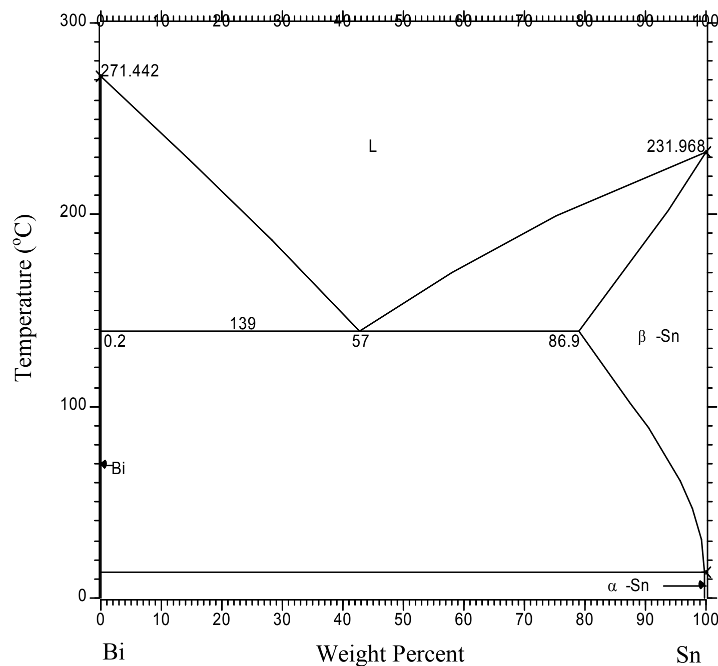

*Figure 2.5.*Bi-Sn phase diagram (Franke & Neuschütz, 2004)

2.7.4 Bi-Cu Phase Diagram

Figure 2.6 shows that the equilibrium phases of the Cu-Bi system are (1) the liquid, miscible in all proportions; (2) Cu, with restricted solubility of Bi; and (3) Bi, with negligible solubility of Cu. The assessed phase diagram for the Cu-Bi system is of the eutectic type with the eutectic point located close to pure Bi (Chakrabarti & Laughlin, 1990).

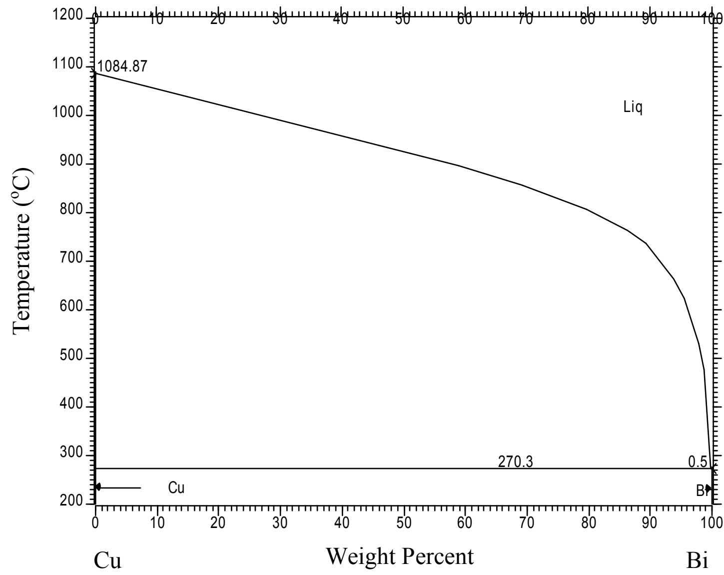

Figure 2.6. Bi-Cu phase diagram (Laughlin, 1990)

2.7.5 Bi-Zn Phase Diagram

The assessment of Okamoto (2000) based on existing experimental results is shown in Figure 2.7. The figure indicates a significant solubility of Zn in (Bi) (few wt% of Zn.

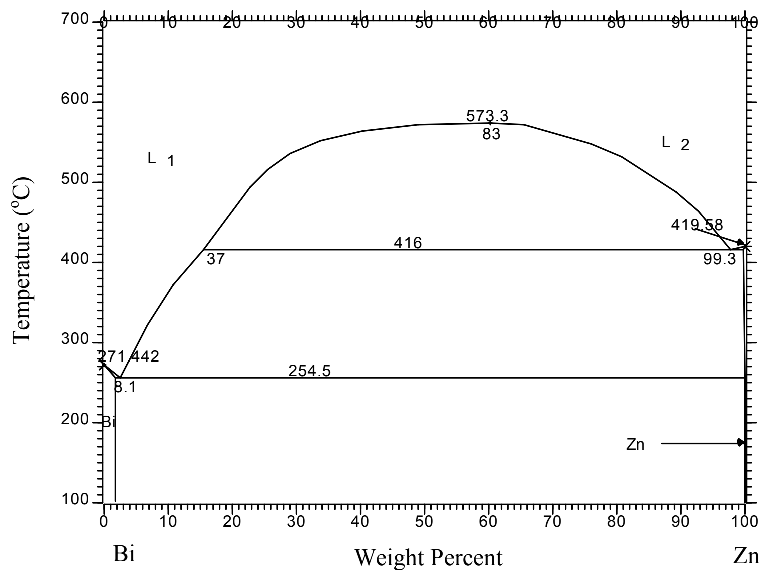

Figure 2.7. Bi-Zn phase diagram (Okamoto, 2000)

2.7.6 In-Sn Phase Diagram

Several In-Sn solder compositions are used in a number of soldering applications, including low-temperature service conditions. The In-Sn system is a binary alloy having an assortment of solid-solution phases. The phase diagram is shown in Figure 2.8. In-Sn system has a eutectic composition of 49.1In-50.9Sn and eutectic temperature of 120 ºC. The eutectic composition is often cited as simply 50In-50Sn. The indium-based solder with the composition of In-48Sn is commonly used for surface mount technology (SMT) applications due to its substantially low melting temperature.

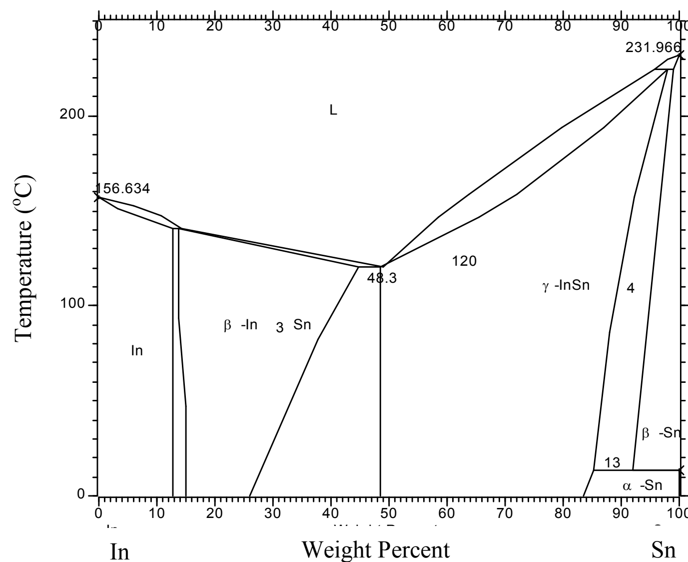

Figure 2.8. In-Sn phase diagram. (Okamoto, 2006)

The two phases formed are intermetallic phases and In-rich, pseudo body centred tetragonal phase, ß, which has 44.8 wt.% Sn, and a hexagonal Sn-rich phase, γ, with 77.6 wt.% Sn (Glazer, 1995). Mei and Morris (1992) described the

microstructure of In-48Sn solder on a Cu substrate as having lamellar features. The Sn-rich phase is composed of equiaxed grains. The In-rich phase contains Sn precipitates.

2.7.7 In-Zn Phase Diagram

Figure 2.9 shows In-Zn phase diagram. The liquidus on the Zn side of the eutectic was calculated, assuming maximum solubility of In in (Zn) to be only 0.12at%In. Liquidus temperatures obtained from the thermodynamic properties are very close to the selected experimental values with an average deviation of ± 6K (Dutkiewicz & Zakulski, 1990).

Tin-zinc eutectic structure consists of two phases: a body centred tetragonal Sn-matix phase and a secondary phase of hexagonal Zn containing less than 1% tin in solid solution (McCormack et al.,1994).

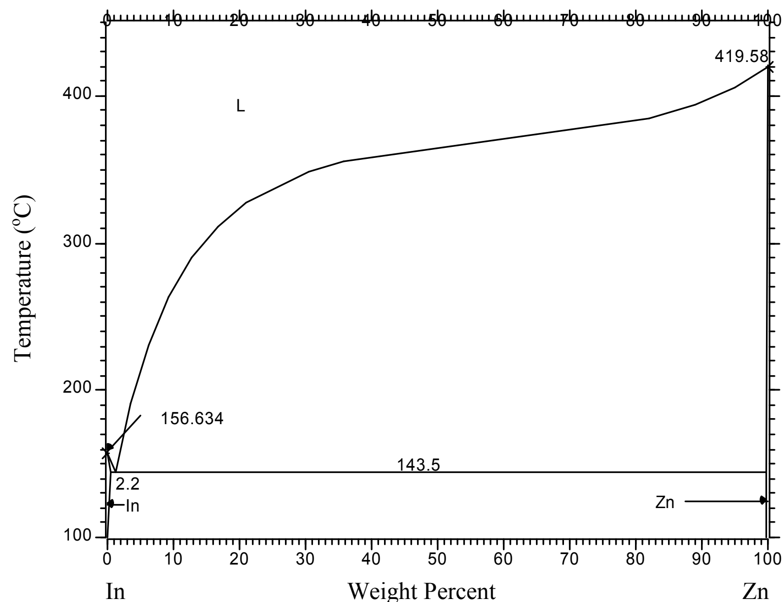

Figure 2.9. In-Zn phase diagram. (Dutkiewicz & Zakulski, 1990)